

Interpretation of the angular dependence of the de Haas-van Alphen effect in MgB₂

A. Carrington and J. D. Fletcher

H. H. Wills Physics Laboratory, University of Bristol, Tyndall Avenue, Bristol BS8 1TL, United Kingdom

H. Harima

Department of Physics, Kobe University, Kobe 657-8501, Japan

(Received 14 December 2004; published 12 May 2005)

We present detailed results for the amplitude and field dependence of the de Haas-van Alphen (dHvA) signal arising from the electronlike π sheet of Fermi surface in MgB₂. Our data and analysis show that the dip in dHvA amplitude when the field is close to the basal plane is caused by a beat between two very similar dHvA frequencies and not a spin-zero effect as previously assumed. Our results imply that the Stoner enhancement factors in MgB₂ are small on both the σ and π sheets.

DOI: 10.1103/PhysRevB.71.174505

PACS number(s): 74.25.Jb, 74.70.Ad

Soon after the discovery of superconductivity in MgB₂, several groups reported calculations of its band structure. The topology of the calculated Fermi surface was verified by measurement of the de Haas-van Alphen (dHvA) effect. The observed^{1,2} dHvA frequencies were in very good agreement with the calculated³⁻⁵ extremal areas on each of the four sheets of Fermi surface. The measured quasiparticle effective masses were also in excellent agreement with the calculated values, providing direct evidence for the predicted large difference in electron-phonon coupling constants between the σ and π bands.

For fields less than 20 T, three dHvA frequencies have much larger amplitude than the others; two of these arise from the minimal and maximal extremal areas of the smaller of the two tubular σ sheets, whereas the third originates from a neck on the electronlike π sheet. In what follows we refer to these dHvA orbits as F_1 , F_2 , and F_3 , respectively (a diagram showing the calculated Fermi surface and predicted dHvA orbits can be found in Ref. 2).

In Ref. 2, it was shown that the angular dependence of the dHvA amplitude for F_1 and F_2 could be adequately explained by the usual Lifshitz-Kosevich expression for the oscillatory torque Γ_{osc} of a three-dimensional (3D) Fermi liquid,⁶ but for F_3 it could not. There were two puzzling features. First, the amplitude of F_3 showed a pronounced dip at $\theta \approx 76^\circ$ (see Fig. 4)⁷ which was attributed to a spin-zero effect. The Stoner enhancement deduced from the position of this dip is approximately two times larger than that predicted⁴ and four times larger than those measured for the σ sheet orbits, F_1 and F_2 . Second, we were unable to explain the angle dependence of the amplitude. In this paper we will present detailed measurements of the field dependent dHvA amplitude of F_3 as a function of angle, and show that the feature previously ascribed to a spin-zero is actually caused by a beat with another dHvA frequency.

Quantum oscillations in the torque produced by a small single crystal of MgB₂, (mass = 5.6 μg) were measured with a piezoresistive, doped silicon cantilever.⁸ The cantilever is mounted on a single axis rotation stage in a ³He cryostat inside the bore of a 19 T superconducting magnet (20.5 T at $T = 2.2$ K). All measurements in this paper were performed in liquid ³He at 320 ± 20 mK. Changes in the resistance of the

cantilever are directly proportional to the torque and were measured using an AC bridge technique.⁹ The torque values are reported here in units of bridge resistance R , i.e., the off-balance voltage divided by the excitation current (the change in lever resistance is 4 times larger than this). We estimate that $\Gamma = 10^{-10}R$ (Γ in Nm and R in Ω). The noise level is around 2 m Ω or $\sim 10^{-13}$ Nm. The crystal of MgB₂ was grown by a high pressure synthesis route⁷ and is the same as sample B in Refs. 1 and 2.

We interpret our data using the standard expression for the first harmonic of the oscillatory part of the torque for a 3D Fermi liquid^{6,10}

$$\Gamma_{\text{osc}} \propto \frac{B^{3/2}}{[\Lambda'']^{1/2}} \frac{dF}{d\theta} R_D R_T R_{SC} R_S \sin\left(\frac{2\pi F}{B} + \varphi\right), \quad (1)$$

where F is the dHvA frequency [$F = (\hbar/2\pi e)\Lambda$, Λ is the extremal orbit area in \mathbf{k} space]; $\Lambda'' = \partial^2 \Lambda / \partial k^2$ is the curvature factor and φ is the phase. R_D , R_T , and R_S are the damping factors from impurity scattering, temperature, and spin splitting, respectively. The Dingle factor, $R_D = \exp(-\pi \hbar k_F / eB\ell)$, where k_F is the orbitally averaged Fermi wave vector^{6,11} and ℓ is the quasiparticle mean free path. The thermal damping factor, $R_T = X / \sinh X$ where $X = (2\pi^2 k_B m^* T) / (\hbar e B)$, m^* is the quasiparticle effective mass. The factor R_{SC} accounts for the additional damping when the sample enters the superconducting state, and was studied in detail in MgB₂ in Ref. 12. The spin splitting factor is given by $R_S = \cos\{[\pi g m_B (1+S)] / (2m_e)\}$ where $1+S$ is the orbitally averaged exchange-correlation (Stoner) enhancement factor, g is the electron g -factor, m_e is the free-electron mass. When $g(1+S) \times (m_B/m_e)$ equals an odd integer, $R_S = 0$ and the spin-up and spin-down Fermi surfaces beat out of phase to produce a spin-zero minimum in the dHvA amplitude. If the location of any of these spin-zeros can be measured, and $m_B(\theta, \phi)$ is known from band-structure calculations, then the Stoner factor on each orbit may be deduced.¹³ Note that R_S does not depend on B , so near to a spin-zero the dHvA amplitude is suppressed at all fields.

Although it is possible to fit the data directly to Eq. (1) it is often more illuminating to extract the field dependent am-

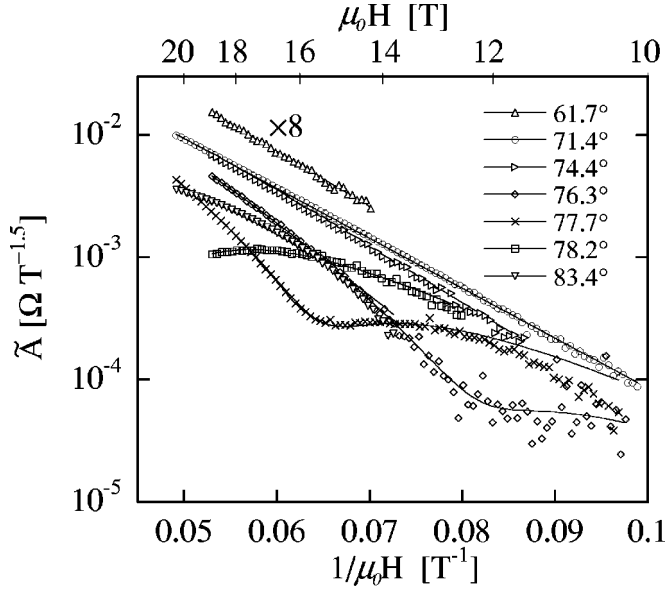


FIG. 1. Reduced dHvA amplitude (\tilde{A}) versus inverse field for several rotation angles. The lines are fits of the data to Eq. (3). The data for $\theta=61.7^\circ$ have been multiplied by 8 for clarity.

plitude A of the dHvA oscillations by fitting small sections of the data (comprising of 1.5 oscillations) to

$$\Gamma_{\text{osc}}(B) = A \sin\left(\frac{2\pi F}{B} + \varphi\right) + aB + b \quad (2)$$

(the linear term accounts for the slowly varying background torque and magnetoresistance of the cantilever). We then divide A by $B^{3/2}R_T$ to give the reduced amplitude \tilde{A} , which in the absence of other effects (i.e., $R_{SC}=1$)¹⁴ is proportional to the Dingle factor R_D . The quasiparticle effective mass m^* in the expression for R_T was determined by measuring the temperature dependence of the dHvA amplitude [for F_3 , $m^* = (0.456 \pm 0.005)m_e$ at $\theta=70.8^\circ$].

In Fig. 1 we show reduced dHvA amplitude \tilde{A} versus inverse field (Dingle plot) for orbit F_3 at selected angles. For $\theta=61.7^\circ$ and 71.4° the behavior is strictly exponential, $\tilde{A} \propto \exp(-\alpha/B)$. However, for $\theta \geq 71.4^\circ$, α appears to increase rapidly and the Dingle curves become markedly nonexponential. The dHvA amplitude is strongly reduced, but unlike the expected behavior close to a spin-zero, the reduction is not uniform at all fields. For $\theta < 72^\circ$ the increase in the coefficient α with decreasing angle is given by $\alpha = (89/\sin \theta) \times \epsilon(\theta)$. The $\sin \theta$ factor arises from the cylindrical nature of this section of Fermi surface (the band mass and the dHvA frequency increase by the same factor). The factor $\epsilon(\theta)$ was determined experimentally by fitting the data for $\theta < 72^\circ$; we find, $\epsilon(\theta) \approx 1 + 3.7(1 - \sin \theta)^2$ reflecting an increase in scattering rate with decreasing θ . From this we estimate the quasiparticle mean free path (at $\theta=0^\circ$) on this orbit to be 660 \AA .

We will show below that the most likely reason for the nonexponential Dingle curves is a beat with a second dHvA frequency. Before we present this analysis in detail we will briefly discuss two other possible explanations.

The background and oscillatory torque cause deflections in the cantilever so the measurements are not performed at strictly constant angle. This torque interaction effect¹⁵ causes spurious generation of harmonics and mixing of frequencies, and because the amplitude is angle dependent it can also cause bending of the Dingle curves. We can quantify this effect by fitting the data to Eq. (1), allowing for the change in dHvA frequency with field. To a good approximation¹ $F_3(\theta) = F_3^0/\sin(\theta)$, and θ is given by the measured angle plus the field dependent deflection of the cantilever, $\theta = \theta_0 + \lambda\Gamma(B)$ (λ is a fitting constant which measures the stiffness of the cantilever). For the data presented here we find that $\lambda \approx 0.04 \text{ degrees}/\Omega$.¹⁶ The result of this analysis is that the torque interaction effect is much too small to explain the nonexponential behavior shown in Fig. 1.

Another possibility stems from a mosaic spread in the direction of the a or c axis of the crystal. Beats between different dHvA frequencies originating from different parts of the crystal can produce nonexponential Dingle curves.¹⁷ The size of the effect depends on the spread of the dHvA frequencies and in the present case would become largest as the field is rotated away from the basal plane. Experimentally we find that curvature in the Dingle plot only occurs for angles close to the basal plane, and therefore conclude that in our crystals the mosaic structure does not play a significant role. This conclusion is reinforced by the fact that the observed behavior is highly reproducible between different crystals.

Simple trigonometric relations show that if two dHvA signals with frequencies F and $F + \Delta F$ and amplitudes in the ratio β (with identical Dingle factors) are added together, and the resultant fitted with a single frequency F then the reduced amplitude \tilde{A} will vary like

$$\begin{aligned} \tilde{A} &= \tilde{A}_0 \exp\left(-\frac{\alpha}{B}\right) D(B) \sin\left(\frac{2\pi F}{B} + \delta(B)\right), \\ D(B) &= \left[1 + \beta^2 + 2\beta \cos\left(\frac{2\pi\Delta F}{B}\right)\right]^{1/2}, \\ \delta(B) &= \tan^{-1}\left(\frac{\beta \sin\left(\frac{2\pi\Delta F}{B}\right)}{1 + \beta \cos\left(\frac{2\pi\Delta F}{B}\right)}\right). \end{aligned} \quad (3)$$

In Fig. 1 we show that these equations provide a very good fit to the reduced dHvA amplitude data. In these fits there are three free parameters, A_0 , ΔF , and β (α was fixed at the values found by extrapolating from lower θ as described above). The variations of ΔF and β with θ are shown in Fig. 2. The frequency difference increases approximately linearly with θ , $\Delta F \approx 1.4(\theta - 70^\circ)$. The data are consistent with β being almost constant as a function of angle and then going rapidly to zero for $\theta \leq 73^\circ$. Note that as $F_3(\theta) \approx 2684/\sin(\theta)$, the maximum value of ΔF corresponds to only $\sim 0.4\%$ difference in $\langle k_F \rangle$ between the two orbits.

A extremal dHvA orbit F_3^* with frequency close to F_3 was predicted from band structure calculations³ and is shown in

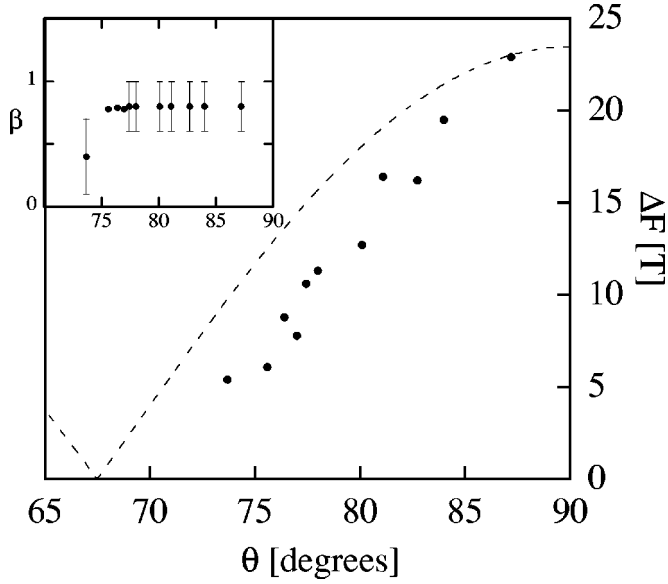


FIG. 2. Variation of the frequency difference ΔF and the relative amplitude β of the beat frequency as a function of θ . The dashed line is Eq. (4), $l^* = 0.12(a^*/\sqrt{3})$ and $\Delta F_0 = 23.5$ T.

Fig. 3. Close to the two extremal orbits this sheet of Fermi surface is tubular, with only slight warping. The difference in dHvA frequency between the extremal orbits of a cylinder with simple cosine warping^{18,19} is given by

$$\Delta F(\theta) = \frac{\Delta F_0}{\sin(\theta)} J_0\left(\frac{\pi k_F}{l^*} \cot(\theta)\right). \quad (4)$$

Here l^* is the k -space distance between the minimum and maximum frequency orbits and J_0 is the Bessel function. For $\theta \geq 65^\circ$, the detailed band structure determination of $\Delta F_3 = F_3^* - F_3$ closely follows this equation with $\Delta F_0 \approx 57$ T, and $l^* \approx 0.13(a^*/\sqrt{3})$ (Ref. 20). For $\theta \leq 65^\circ$, $\Delta F_3(\theta) = 0$, i.e., only

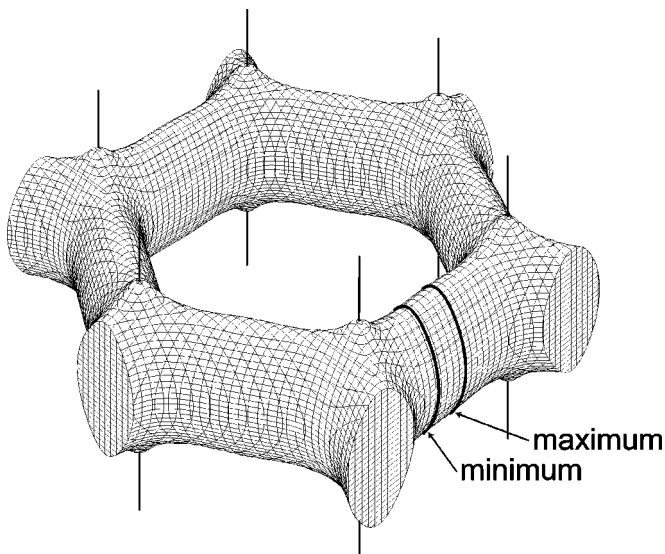


FIG. 3. The calculated electronlike π band Fermi surface sheet of MgB_2 , showing the location of the two F_3 dHvA orbits.

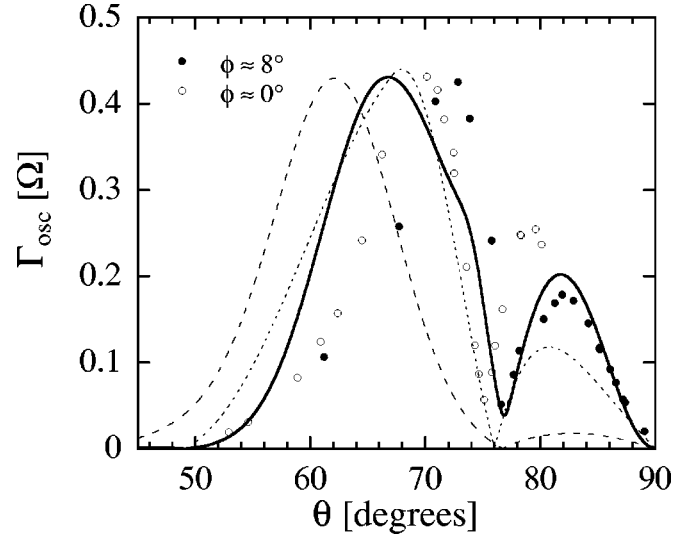


FIG. 4. Experimental dHvA torque amplitude versus θ at fixed field ($17.8T < B < 18.0T$) for orbit F_3 . Data for two different in-plane rotation angles ϕ are shown. Fits to the two frequency model [Eq. (3)], warped cylinder model [Eq. (5)], and single frequency model [Eq. (1)] are shown by the solid, dotted, and dashed, lines respectively.

one extremal orbit is found. This reflects a difference between the actual Fermi surface topology and the cosine dispersion which leads to Eq. (4). The characteristics of this predicted second orbit closely match our observations. The only significant difference is that the maximum frequency difference we find is around half the predicted value (i.e., the cylinder is actually somewhat less warped than the calculation). Experimentally, the Dingle curves are straight for $\theta \leq 72^\circ$ (Fig. 1), showing that the second orbit is absent for $\theta \leq 72^\circ$ in approximate agreement with the detailed calculation.

We conclude that the dip in amplitude for orbit F_3 is caused by a beat effect and not a spin-zero as previously assumed. From the data in Fig. 4 it seems likely that any spin-zero would have to occur for $\theta < 50^\circ$ and hence [assuming for F_3 , $m_B \propto (\sin \theta)^{-1}$] the Stoner enhancement factor on this orbit is less than 0.22. A summary of all the Stoner factors derived from dHvA measurements is shown in Table I (the values for F_1 and F_2 are taken from a previous study² on a different MgB_2 crystal²¹). The enhancement factors on both the σ and π sheets are somewhat smaller than calculations⁴ would suggest. By comparing measurements of the Pauli susceptibility, derived from conduction electron spin resonance experiments, to band-structure calculations of the total density of states at the Fermi level, Simon *et al.*²²

TABLE I. Summary of measured ($1+S_{\text{exp}}$) and calculated (Ref. 4) ($1+S_{\text{calc}}$) Stoner enhancement factors for the three orbits.

Orbit	Sheet	$1+S_{\text{exp}}$	$1+S_{\text{calc}}$
F_1	σ_1	1.07	1.31
F_2	σ_1	1.12	1.31
F_3	π_1	<1.22	1.26

found that $1+S$ (averaged over all Fermi surface sheets) was 0.86 ± 0.13 , i.e., the average enhancement is small in agreement with our findings.

Using the measured values of α , $\Delta F(\theta)$, and $\beta(\theta)$ along with the calculated curvature factor A'' , we are able to calculate the expected angular dependence of the dHvA amplitude at fixed field using Eq. (1). Here we have fixed the constant of proportionality in Eq. (1) to match the maximum in the experimental data, and we have also fixed $1+S=1.2$. As mentioned above, $1+S$ must be $\lesssim 1.22$ and values less than 1.2 do not change the curve markedly. The agreement between the calculation and the data is good, although not perfect. Importantly, the calculation reproduces the key dip feature at $\theta \approx 76^\circ$.

Actually, for such a flat portion of Fermi surface, the usual LK expression [Eq. (1)] should be modified as the usual integral over the tube is no longer strongly peaked at the extremal orbits. For a simple cosine dispersion the curvature factor is replaced by^{19,23}

$$R_Y = J_0 \left(\frac{\pi \Delta F(\theta)}{B} \right). \quad (5)$$

A fit to the amplitude data with Eqs. (4) and (5) is shown as the dotted line in Fig. 4. Here we have set $l^* = 0.12(a^*/\sqrt{3})$ and $\Delta F_0 = 23.5T$ to best fit both the $\Delta F(\theta)$ and $\Gamma_{\text{osc}}(\theta)$ data. The fit again reproduces the main features of the experimental data but is slightly worse than the discrete frequency fit. It can be seen (Fig. 2) that the experimentally determined $\Delta F_3(\theta)$ data does not quite follow Eq. (4), showing that the

true local warping is not quite sinusoidal. The behavior below $\theta = 74^\circ$, where the second frequency is not detected experimentally, is particularly badly described by this approximation. In principle, the fit could be improved by using the actual band-structure determined Fermi surface data in Fig. 3 however, unfortunately the numerical accuracy of this data is insufficient to do this to the required precision.

The dashed line in Fig. 4 shows the behavior expected without the beat effect but with $1+S=1.545$, which is required to produce a spin-zero dip at the same angle. Clearly the correspondence with the data is much worse, especially for angles close to the basal plane.

For the series of sweeps reported in Figs. 1 and 2, the in-plane angle ϕ was estimated to be $\sim 8^\circ$. A second (less extensive) set of runs with $\phi \approx 0^\circ$ shows very similar behavior. The main difference is that the dip occurs at lower θ (see Fig. 4). Repeating the above analysis on this set of data again shows a linear θ dependence of ΔF but with a larger slope, $d\Delta F/d\theta \approx 1.9$ T/degree. If we use this value in our calculation we find the dip moves to lower θ , in accord with the experimental data.

In summary, we have shown that the dip in the dHvA amplitude for fields aligned close to the basal plane of MgB_2 is due to a beat between two very similar dHvA frequencies and not a spin-zero effect as previously assumed. The data imply that the Stoner enhancement factors on both the σ and π sheets of Fermi surface are small.

The authors thank J. R. Cooper for useful discussions and S. Lee and S. Tajima for supplying the single crystals of MgB_2 .

¹E. A. Yelland, J. R. Cooper, A. Carrington, N. E. Hussey, P. J. Meeson, S. Lee, A. Yamamoto, and S. Tajima, *Phys. Rev. Lett.* **88**, 217002 (2002).

²A. Carrington, P. J. Meeson, J. R. Cooper, L. Balicas, N. E. Hussey, E. A. Yelland, S. Lee, A. Yamamoto, S. Tajima, S. M. Kazakov, and J. Karpinski, *Phys. Rev. Lett.* **91**, 037003 (2003).

³H. Harima, *Physica C* **378**, 18 (2002).

⁴I. I. Mazin and J. Kortus, *Phys. Rev. B* **65**, 180510(R) (2002).

⁵H. Rosner, J. M. An, W. E. Pickett, and S. L. Drechsler, *Phys. Rev. B* **66**, 024521 (2002).

⁶D. Shoenberg, *Magnetic Oscillations in Metals* (Cambridge University Press, Cambridge, 1984).

⁷Here, θ is the angle between the field and the c axis as the sample is rotated towards the basal plane. The in-plane direction we are rotating towards is denoted by ϕ (measured from the a axis).

⁸Veeco Instruments, Inc., Woodbury, New York; <http://www.veeco.com>.

⁹J. R. Cooper, A. Carrington, P. J. Meeson, E. A. Yelland, N. E. Hussey, L. Balicas, S. Tajima, S. Lee, S. M. Kazakov, and J. Karpinski, *Physica C* **385**, 75 (2003).

¹⁰Note that in Ref. 2 the exponent of B in Eq. (1) is wrongly given as $\frac{1}{2}$.

¹¹A. Wasserman and M. Springford, *Physica B* **194**, 1801 (1994).

¹²J. D. Fletcher, A. Carrington, S. M. Kazakov, and J. Karpinski, *Phys. Rev. B* **70**, 144501 (2004).

¹³The g factor in MgB_2 has been measured to be very close to 2—see Ref. 22.

¹⁴As discussed in Ref. 12, the data in Fig. 1 are taken at sufficiently high fields so that the effect of superconductivity can be neglected (except possibly for $\theta = 77.7^\circ$ and $1/\mu_0 H \gtrsim 0.09$).

¹⁵C. Bergemann, S. R. Julian, A. P. Mackenzie, A. W. Tyler, D. E. Farrell, Y. Maeno, and S. Nishizaki, *Physica C* **318**, 444 (1999).

¹⁶We find that this parameter can vary by up to a factor of 4 between different cantilevers from the same supplier.

¹⁷R. J. Higgins and D. H. Lowndes, in *Electrons at the Fermi Surface*, edited by M. Springford (Cambridge University Press, Cambridge, 1980).

¹⁸K. Yamaji, *J. Phys. Soc. Jpn.* **58**, 1520 (1989).

¹⁹Y. Yoshida, A. Mukai, R. Settai, K. Miyake, Y. Inada, Y. Onuki, K. Betsuyaku, H. Harima, T. D. Matsuda, Y. Aoki, and H. Sato, *J. Phys. Soc. Jpn.* **68**, 3041 (1999).

²⁰ a^* is the in-plane reciprocal lattice vector and $a^*/\sqrt{3}$ is the length of one side of the hexagonal Brillouin zone.

²¹For the present crystal the scattering rate on the σ sheet orbits is too large to observe the dHvA signal at sufficiently large angle for the spin-zero to be observed.

²²F. Simon, A. Janossy, T. Feher, F. Muranyi, S. Garaj, L. Forro, C. Petrovic, S. L. Bud'ko, G. Lapertot, V. G. Kogan, and P. C. Canfield, *Phys. Rev. Lett.* **87**, 047002 (2001).

²³C. Bergemann, S. R. Julian, A. P. Mackenzie, S. Nishizaki, and Y. Maeno, *Phys. Rev. Lett.* **84**, 2662 (2000).